# Cellular gp96 upregulates AFP expression by blockade of NR5A2 SUMOylation and ubiquitination in HCC

Liyuan Qian[1], Zhentao Liang[1,2] , Zihao Wang[1,2], Jiuru Wang[1,2], Xin Li[1], Jingmin Zhao[3,] Zihai Li[4,] Lizhao Chen[1], Yongai Liu[1,2],Ying ju[1], Changfei Li[1*], Songdong Meng[1,2*]

1 Key Laboratory of Pathogen Microbiology and Immunology, Institute of Microbiology, Chinese Academy of Sciences，Beijing, 100101,China.

2 University of Chinese Academy of Science, Beijing, 100049, China.

3 Department of Pathology and Hepatology, the fifth Medical Centre, Chinese PLA General Hospital, Beijing, 100039, China.

4 Pelotonia Institute for Immuno-Oncology, the Ohio State University Comprehensive Cancer Center - the James, Columbus, OH, 43210, United States.

Corresponding author: Songdong Meng (mengsd@im.ac.cn), Changfei Li lichangfei2006@163.com)

## Abstract

AFP is the most widely used biomarker for the diagnosis of hepatocellular carcinoma. However, a substantial proportion of HCC patients have either normal or marginally increased AFP levels in serum, and the underlying mechanisms are not fully understood. In the present study, we provided *in vitro* as well as *in vivo* evidence that heat shock protein gp96 promoted AFP expression at the transcriptional level in HCC. NR5A2 was identified as a key transcription factor regulated by AFP and its stability was enhanced by gp96. A further mechanistic study by CO-IP, GST-pull down and molecular docking showed the competitive binding of gp96 and SUMO E3 ligase RanBP2 to NR5A2 at the sites spanning from aa 507 to 539. The binding of gp96 inhibited SUMOylating, ubiquitination, and subsequent degradation of NR5A2. In addition, clinical analysis of HCC patients indicated that gp96 expression was

positively correlated to serum AFP levels in tumors. Therefore, our study uncovered the novel regulatory mechanism of gp96 on the stability of its client proteins by directly affecting their SUMOylation and ubiquitination. These findings will help in designing more accurate AFP-based HCC diagnosis and progression monitoring approaches.

**Keywords:** Gp96, AFP, NR5A2, RanBP2, SUMOylation

## Introduction

Alpha-fetoprotein , a 70 kDa glycoprotein, is the main serum protein produced during fetal life(Deutsch, 1991). Unlike other members of the serum-albumin family, the AFP gene is transcriptionally silent in the adult liver but is reactivated in hepatocellular carcinoma (HCC), where elevated serum levels of AFP have been found in about 70-85% of HCC patients(Galle et al., 2019). Since serum AFP is mainly produced by hepatic tumor cells, a concentration of 20 ng/mL is generally used as a pathological threshold value, and > 400 ng/mL is usually considered diagnostic for HCC(Sauzay et al., 2016; Galle et al., 2019). Although the discovery of new oncologic markers has been carried out for decades, AFP remains the most widely used biomarker in HCC diagnosis(Sauzay et al., 2016; Galle et al., 2019).

Several underlying regulatory mechanisms of pathological AFP expression have been reported in HCC(Sauzay et al., 2016). Numerous transcription factors are crucial for the regulation of the AFP promoter(Kajiyama et al., 2006; Peterson et al., 2011; Sauzay et al., 2016). The human AFP gene is comprised of five regulatory regions: a tissue-specific promoter, a repressor upstream of the promoter, and the three enhancers located at 2.5, 5.0, and 6.5 kb upstream of the AFP promoter, respectively(Bernier et al., 1993; Sauzay et al., 2016). The potential AFP transcription factors include hepatocyte nuclear factor-1 (HNF-1), liver receptor homolog-1 (LRH-1, also known as FTF or NR5A2), retinoid x receptor (RXR), CAAT/enhancer binding protein (C/EBP), homeobox protein NK-2 (Nkx2.8), zinc-fingers and

homeoboxes 2 (Zhx2), and zinc finger and BTB domain containing 20 (Zbtb20)(Bernier et al., 1993; Kajiyama et al., 2006; Peterson et al., 2011; Sauzay et al., 2016). Zhx2 and Zbtb20 bind specifically to the AFP promoter and inhibit its activity; their levels are increased with the decrease in AFP expression after birth(Xie et al., 2008; Peterson et al., 2011). AFP expression could also be regulated post-transcription by miRNAs including miRNA-122, miRNA-620, miRNA-1236, miRNA-1270, and miRNA-329, which directly target the 3'-UTR region of the AFP mRNA(Kojima et al., 2011; Gao et al., 2015). In addition, epigenetic regulation like methylation, and acetylation status of the AFP gene also influence AFP expression(W. Chen et al., 2020; Xue et al., 2020). Nevertheless, serologic surveillance showed that a significant proportion (around 15-30%) of HCC patients have either normal or minimally increased AFP levels(Gurakar et al., 2018). Meanwhile, other liver diseases such as hepatitis and cirrhosis may also lead to elevated serum AFP levels. Therefore, the exact mechanisms of AFP expression in HCC are not well understood and need further investigation(Sauzay et al., 2016; Galle et al., 2019).

Heat shock protein (HSP) gp96 is the most abundant protein in the endoplasmic reticulum (ER)(B. X. Wu et al., 2016). Similar to most of HSPs, gp96 acts as a molecular chaperone in protein folding and facilitates the degradation of misfolded proteins. Unlike its cytosolic counterpart *HSP90*, gp96 has a relatively strict binding selectivity and only binds certain client proteins, including Toll receptor (Toll-like receptors), the majority of α and β integrin subunits, Wnt co-receptor low-density lipoprotein receptor-related protein 6, glycoprotein A repetitions predominant, insulin-like growth factor, binding immunoglobulin protein (BiP), epidermal growth factor receptor-2 (HER2), and uPAR(B. Liu et al., 2010; Hong et al., 2013; Hou et al., 2015b; Li et al., 2015; B. Wu et al., 2015; Ansa-Addo et al., 2016; Marzec et al., 2016; B. X. Wu et al., 2016; Duan et al., 2021). These client proteins are involved in balancing cancer-induced ER stress responses and regulating inflammation in the tumor microenvironment(Marzec et al., 2012). An elevated level of gp96 correlates with the development, invasion, and metastasis of tumors, which validates the

pro-oncogenic function of cellular gp96(Hou et al., 2015b; Li et al., 2015; B. Wu et al., 2015; Ansa-Addo et al., 2016; B. X. Wu et al., 2016; Duan et al., 2021). Furthermore, cellular and cell membrane gp96 has been shown to promote anti-apoptotic characteristics and metastasis of HCC via interaction with p53 and uPAR concluding the association of high gp96 expression with tumor metastasis and recurrence(Hou et al., 2015b; B. Wu et al., 2015; Cho et al., 2022; Pugh et al., 2022).

The present study aimed to comprehensively examine the effects of gp96 on AFP expression and its serum levels in HCC by generating hepatic gp96 knock-out mice and clinical sample analysis. The underlying mechanism of the gp96-mediated regulatory network was further dissected. The results uncovered a novel regulatory pathway of AFP expression and suggested that detection of gp96 levels may increase the sensitivity of HCC diagnosis by AFP test.

## Results

### Hepatic knock-out of gp96 dramatically decreases AFP levels in DEN-induced HCC

In this study, we used the well-established DEN-induced HCC mouse model, where liver-specific gp96KO mice and Het mice were intraperitoneally injected with DEN to induce hepatic tumors (Rachidi et al., 2015). Deletion of gp96 (*Hsp90b1*) in the liver of gp96KO mice was confirmed by Real-time PCR and Western blotting (Figure 1A)(Rachidi et al., 2015). Eight months after DEN-injection, both gp96KO and Het mice developed visible liver tumors; tumor histological features were shown by H&E staining (Figure 1B)(Rachidi et al., 2015). Compared to the DEN-untreated Het mice liver tissue, there was a drastic increase in gp96 and AFP levels in DEN-induced liver tumors (Figure 1C). Consistent with a previous study, fatty nodules were observed in tissue sections of gp96KO mice tumors (Supplementary Figure S1A)(Rachidi et al., 2015). Gp96KO mice showed a decrease in tumor weight and low tumor burden compared to Het mice under DEN treatment (Figure 1D). Global gene expression in liver tumor tissues of gp96KO and Het mice was studied by

transcriptome analysis. Compared to the Het group, gp96KO mice showed increased expression of 5413 genes and decreased expression of 4488 genes in HCC (Figure 1E, and Additional file 1; fold change (log2FC) > 0.5), among which AFP expression was reduced by around 2.488-fold. The decrease in AFP gene expression was confirmed by Real-time PCR (Figure 1F), Western blotting (Figure 1G), and IHC analysis (Figure 1H).

**Cellular gp96 promotes AFP expression mainly through its transcription factor NR5A2 in hepatoma cells**

Two hepatoma cells, Huh7 and HepG2, with stable knockdown of gp96 were used to determine gp96-mediated AFP expression. Compared to the mock, knockdown of gp96 caused an obvious decrease in AFP mRNA as well as protein levels (Figure 2A and B). In the meantime, gp96 knockdown also caused a pronounced decrease in AFP levels by 98% and 95% in the supernatant of Huh7 and HepG2 cells, respectively (Figure 2C). In contrast, overexpression of gp96 in Huh7 cells resulted in increased levels of cellular AFP mRNA and protein (Figure 2D and E), as well as elevated AFP secretion (Figure 2F). Overall, the data suggested that gp96 promotes AFP expression at the transcriptional level.

**The effect of gp96 on the expression of AFP transcription factors**

The potential binding sites of AFP transcription factors in the promoter region are shown in Figure 3A (Bernier et al., 1993; Kajiyama et al., 2006; Peterson et al., 2011; Sauzay et al., 2016). As seen in Figure 3B and C, knockdown of gp96 caused a sharp decrease in HNF1, HNF4, and C/EBPα, but an increase in Nkx2.8 mRNA as well as protein levels. For NR5A2, gp96 knockdown only decreased its protein level but did not affect its mRNA level (Figure 3B and C). Furthermore, an AFP promoter luciferase reporter assay was performed to determine the key transcriptional factors involved in gp96-induced AFP expression. Compared to the wild-type promoter,

mutations within the binding sites of Nkx2.8 or NR5A2/HNF4 significantly suppressed the AFP promoter activity in Huh7 cells. In addition, mutations within the binding sites of HNF1 also led to a slight decrease in AFP promoter activity. Gp96 knockdown-induced decrease in promoter activity was only mildly affected by mutations in HNF1 binding sites but was abolished by mutations in Nkx2.8 or NR5A2/HNF4 binding sites (Figure 3D and E).Nkx2.8, NR5A2 and HNF4 were then selected for RNAi treatment. Only NR5A2 siRNA treatment largely abolished the effect of gp96 knockdown on promoter activity. Decrease of AFP expression induced by gp96 knockdown was inhibited by NR5A2 siRNA treatment(Figure 3F, G and Supplementary Figure S2). Collectively, these data suggested that cellular gp96 regulates AFP expression mainly via NR5A2.

**Cellular gp96 interacts with NR5A2 and enhances its stability**

Next, the effect of gp96 on the expression of NR5A2 was determined. A sharp increase in protein level (around 3.6 folds) but not in mRNA level of NR5A2 was detected in gp96 transfected Huh7 cells compared to mock (Figure 4A and B). In addition, the gp96-mediated increase in NR5A2 levels was gp96 dose-dependent (Figure 4C). Conversely, a drastic reduction of 87% in NR5A2 protein level but not mRNA level was observed in Huh7-gp96KD cells (Figure 4D and E). Decreased NR5A2 protein levels were also observed in DEN-induced liver tumors of gp96KO mice (Supplementary Figure S3)(Rachidi et al., 2015). As seen in Fig. 4f, the knockdown of gp96 caused a dramatic reduction in the protein stability of NR5A2.

As illustrated in Figure 4G, the co-IP assay showed that endogenous gp96 is associated with NR5A2 in Huh7 cells. To identify the interaction regions between gp96 and NR5A2, GST-tagged full-length gp96, its N-terminal, M-domain, and C-terminal domain fragments, GST-NR5A2, and His-gp96 were expressed (Supplementary Figure S4A-C). GST pull-down assay demonstrated that the full-length gp96 and its C-terminal domain were able to interact with NR5A2 (Figure 4H). Meanwhile, the GST-tagged NR5A2 pull-down assay also indicated a direct

interaction between gp96 and NR5A2 (Figure 4I and J). The whole Immunoblotting membrane of all IP data has been supplied in Additional file 4.

**Cellular gp96 inhibits the interaction of RanBP2 with NR5A2 and reduces RanBP2-mediated NR5A2 SUMOylation and subsequent ubiquitination**

Knockdown of gp96 in Huh7 cells significantly increased NR5A2 ubiquitination, while gp96 overexpression suppressed the ubiquitination dramatically (Figure 5A). Since, post-transcriptional processing in nuclear receptors of the NR5A subfamily mainly occurs via the SUMOylated modification, we quantified SUMO1, SUMO2/3, and their related conjugates(W. Liu et al., 2021a). Our results showed that knockdown or overexpression of gp96 in Huh7 cells affected protein SUMOylation via SUMO1 but not via SUMO2/3 (Supplementary Figure S5A and B and). Also, knockdown of gp96 promoted NR5A2 SUMOylation by SUMO1 modification, whereas overexpression of gp96 inhibited its SUMOylation (Figure 5B). Moreover, gp96 knockdown-induced NR5A2 ubiquitination was highly attenuated by SUMO1 siRNA (Figure 5C and Supplementary Figure S5C), suggesting that SUMO1 SUMOylation is involved in NR5A2 ubiquitination.

To identify a potential SUMO1 E3 ligase, mass spectrometry (LC-MS/MS) was performed on NR5A2-associated proteins (Additional file 2). Among the detected proteins, nucleoporin RanBP2 has been reported to possess SUMO1 E3 ligase activity(Pichler et al., 2002; Reverter and Lima, 2005). The results of the co-IP assay validated the interaction of NR5A2 with RanBP2 (Figure 5D). Moreover, compared with wild type NR5A2, mutation of SUMO interacting motif (SIM) within NR5A2 almost removed its SUMOylation by SUMO1 (Figure 5E), suggesting that the SUMO1 E3 ligase of RanBP2 is SIM-dependent. It was found that their interaction was enhanced in gp96 knockdown cells, whereas it was suppressed by gp96 overexpression (Figure 5F). Unlike NR5A2, gp96 knockdown did not affect RanBP2 levels (Supplementary Figure S6). Similarly, gp96 knockdown increased the SUMOylation of NR5A, and RanBP2 RNAi inhibited this effect (Figure 5G and

Supplementary Figure S5D). Cellular gp96 inhibited the interaction of NR5A2 with RanBP2 in a dose-dependent manner (Figure 5H). GST pull-down assay further demonstrated that gp96 was competitively binding against RanBP2 to NR5A2 in a dose-dependent manner (Figure 5I and J).

We obtained similar results for SUMO modification of another RanBP2 substrate, DNA topoisomerase 2-alpha (TOP2A), to which gp96 showed binding (Supplementary Figure S7A-C and S7E)(Dawlaty et al., 2008). In contrast, such regulation was not observed for histone deacetylase 4 (HDAC4), a RanBP2 substrate, which could not bind to gp96 (Supplementary Figure S7A, B, D and F)(Kirsh et al., 2002). Altogether, our results indicated that cellular gp96 interacts with its client protein NR5A2, which might specifically block the binding of its SUMO1 E3 ligase RanBP2, thereby suppressing the RanBP2-mediated SUMOylation and subsequent ubiquitination of NR5A2. The whole Immunoblotting membrane of IP data has been supplied in Additional file 4.

**The binding sites overlap for gp96 and RanBP2 in NR5A2**

Next, molecular docking was performed with ZDOCK Server (version 3.0.2) to crystal structures obtained from PDB(Pierce et al., 2011). The structural model of full-length NR5A2 has a highly conserved DNA binding domain (DBD), a conserved 12-α-helical bundle ligand-binding domain (LBD), and a SUMO-interactive motif (SIM)(Seacrist et al., 2020; W. Liu et al., 2021a). NR5A2-LBD (299-536) was docked and modeled in complex with gp96 (aa 48-754) or RanBP2 (aa 2631-2711) (Figure 6A and B) (Additional file 3) (Huck et al., 2017; Seacrist et al., 2020). It was found that the potential binding sites for gp96 and RanBP2 in NR5A2 span from aa 507 to aa 536 (Figure 6C). As shown in cartoon Figure 6D, gp96 interacts with the region of aa 515-536 of NR5A2 and RanBP2 binds to the region of aa 507-536, These two regions in NR5A2 were highly overlapped. Both Co-IP and His-pull down assays demonstrated that truncated NR5A2 (aa 299-506Δ507-536), with depletion of the binding sites, lost its capacity to interact with gp96 or RanBP2 (Figure 6E-G and Supplementary Figure S8). These data verified that the aa 507-536 sequence of

NR5A2 is necessary for its binding to both gp96 and RanBP2. The whole Immunoblotting membrane of IP data in the Figure has been supplied in Additional file 4.

**High gp96 expression in liver tumors correlates with serum AFP levels in HCC patients**

To address the clinical correlation of gp96 expression in tumor tissue and serum AFP in HCC patients, we analyzed gp96 expression in 63 primary liver tumors by IHC (Figure 7A). IHC staining of intracellular gp96 in liver tissues was shown as faint/medium/strong and qualitatively scored as categories 1+/2+/3+, respectively(Hicks and Tubbs, 2005). As seen in Figure 7B, gp96 expression levels were positively correlated with serum AFP levels in HCC patients ($R^2 = 10.177$; $P = 0.001422$). In addition, patients with elevated gp96 expression also displayed higher serum AFP levels (all $P < 0.01$ among patients with gp96 expression of categories 1+, 2+, and 3+) (Figure 7C).

## Discussion

In this study, we investigated the regulation of AFP expression by gp96 in HCC. Firstly, comparative transcriptome analysis of DEN-induced tumors obtained from the liver of gp96KO and Het mice showed that cellular gp96 increased AFP expression and supported tumor formation. Next, the mechanistic study revealed that gp96 upregulated NR5A2 at the protein level, which is a key transcription factor for the AFP gene. Further, RanBP2 was identified as an NR5A2-associated protein having the SUMO1 E3 ligase activity, and gp96 could block their interaction by competitively binding to the same site in NR5A2. Finally, the clinical data from HCC patients showed that gp96 expression in the tumor was positively correlated with the AFP levels in serum. Figure 8 illustrates the gp96-NR5A2-RanBP2 regulatory pathway that elevates AFP expression in HCC. According to this model, RanBP2

promotes the ubiquitination and proteasomal degradation of NR5A2 by SUMOylation in normal liver tissue and certain HCC with low cellular gp96 expression, thereby halting the NR5A2-induced AFP expression. On the contrary, in HCC with high gp96 expression, gp96 increases AFP transcription by blocking the interaction between NR5A2 and RanBP2. Our results provide new insight into understanding the distinct status of AFP expression in HCC and might help to design AFP-based HCC diagnosis and disease monitoring approaches with enhanced sensitivity and specificity.

NR5A2 (also known as LRH-1and FTF) is a member of the nuclear receptors NR5A subfamily(Fayard et al., 2004; Sun et al., 2021). It contains several lysine residues that are modified with SUMOylation by E3-SUMO ligases(Lee et al., 2016; W. Liu et al., 2021a). SUMOylation regulates the transcriptional activity and subnuclear localization of NR5A2. SUMO modification might also regulate the stability of the transcription factors by affecting the subsequent ubiquitination process through cross-talk with ubiquitin(Lee et al., 2016; Rosonina et al., 2017). However, SUMO E3 ligases involved in the SUMOylation of NR5A2 are still unknown. In our present study, we demonstrated that RanBP2 acts as a SUMO E3 ligase that binds to and target NR5A2 for SUMOylation modification. We further defined its binding site in NR5A2. RanGAP, HDAC4, and Borealin proteins (TOP2A) have been reported as the SUMOylation targets of RanBP2 in previous studies(Kirsh et al., 2002; Dawlaty et al., 2008; Werner et al., 2012). Since, all the identified RanBP2 target proteins, including RanGAP, HDAC4, TOP2A, and NR5A2 are closely associated with cancer development and progression, the exact role of RanBP2 in HCC deserves further investigation(X. Liu et al., 2020; Blondel-Tepaz et al., 2021; X. Liu et al., 2021b).

Heat shock protein gp96 belongs to the *HSP90* family and is a major chaperone protein in the ER(Marzec et al., 2012). Gp96 acts as a master ER chaperone in response to stress, inflammation, and cancer(B. X. Wu et al., 2016; Hoter et al., 2018; Duan et al., 2021). It binds to a variety of client proteins facilitating their folding and directing their maturation, assembly, and export from the ER to the cell surface(Marzec et al., 2012; Kim et al., 2021; Cho et al., 2022). It plays a critical role

in maintaining ER homeostasis and protein quality control(Marzec et al., 2012). In addition, ER-resident gp96 can be translocated to the cell membrane or cytosol(Marzec et al., 2012; B. Wu et al., 2015; Kim et al., 2021). This may be due to decreased expression of KDELR1 that is essential for the retention of gp96 in the ER, which may result in the release of ER-resident gp96 to the cytoplasm or cell membrane(Hou et al., 2015b). We and others found that cell membrane or cytosolic gp96 binds to and stabilizes multiple cancer-related proteins, including pro-ADAMTS9, uPAR, HER2, EGFR, ER-α36, and p53, thereby promoting tumor growth, anti-apoptosis, and invasion(Koo and Apte, 2010; Hou et al., 2015a; Hou et al., 2015b; Li et al., 2015; B. Wu et al., 2015; Duan et al., 2021; Niu et al., 2021). In this study, we uncovered the underlying mechanism of gp96-mediated interaction and stabilization of NR5A2 by sterically blocking the SUMO E3 ligase RanBP2 binding to NR5A2, and protecting SUMOylation-induced NR5A2 degradation. We consider that interaction between gp96 and NR5A2 occurs in the cytoplasm, as NR5A2 exists in both the nucleus and cytoplasm, and Ranbp2 is localized at the cytoplasmic periphery of the nuclear pore complex(Delphin et al., 1997; Shi et al., 2018). A similar regulatory mechanism by gp96 was also observed for TOP2A, which is a RanBP2 substrate as well as gp96 client protein. However, this regulatory mechanism was not observed for HDAC4, which is a RanBP2 substrate but does not interact with gp96. Since ubiquitin and SUMO-related modifications determine the fate of modified proteins, including their proteasomal degradation, it is worthwhile to explore the effects of gp96 on the stability of its client proteins. We found that gp96 directly controls the interaction between the bound proteins and their E3 ubiquitin/SUMO ligases via the same or overlapped binding sites.

Cellular gp96 expression is controlled mainly by heat shock transcription factors (HSFs), e.g., ATF4(Q. Fan et al., 2014). Our previous study found that HBV x protein (HBx) could increase gp96 expression by enhancing the binding of NF-KB to the gp96 promoter(H. Fan et al., 2013). Expression of gp96 increases in malignant hepatocytes with the progression of HCC(H. Fan et al., 2013). Higher levels of gp96

in tumors are associated with intrahepatic metastasis, degree of tumor differentiation, tumor size, and poor survival of patients(W. T. Chen et al., 2014; Ji et al., 2019). High expression of cell membrane gp96 in tumors correlates with pathogenesis and poor prognosis of HCC in patients(Hou et al., 2015b). These studies indicate the potential of gp96 as a prognostic indicator for HCC. Simultaneously, AFP expression levels also increase with the progression of HCC(Sauzay et al., 2016; Galle et al., 2019). AFP levels in serum have been correlated with HBV infection, tumor size, poor differentiation, and invasion of blood vessels(Sauzay et al., 2016; Galle et al., 2019; Zheng et al., 2020). HCC patients with tumor metastasis have the highest levels of serum AFP(Trevisani et al., 2001; Piñero et al., 2020). Thus, it can be concluded that AFP has a close association with the poor prognosis of HCC in patients(Berry and Ioannou, 2013; Sauzay et al., 2016; Galle et al., 2019). The identified AFP transcription factors include NR5A2, Nkx2.8, and RAR, while transcriptional repressors include ZHX2 and ZBTB20(Kajiyama et al., 2006; Peterson et al., 2011; Sauzay et al., 2016). In the present study, we demonstrated that gp96 upregulates AFP gene expression via NR5A2-induced transcription. Clinical data of HCC patients showed that AFP levels in serum are positively correlated with gp96 expression in tumor tissues, and the majority of HCC patients with low gp96 expression exhibited normal AFP levels (see Figure 7). Hence, we tentatively defined two distinct HCC subtypes: low gp96 expression with normal AFP, and high gp96 expression with elevated AFP. This finding indicates that low gp96 expression in liver tumors attributes to normal or minimally increased AFP levels in a substantial proportion of HCC patients.

In conclusion, the current study uncovered a novel mechanism of gp96-mediated upregulation of AFP transcription and expression via NR5A2 in HCC. This mechanism involves the binding of cellular gp96 to NR5A2 and sterically blocking the interaction between NR5A2 and RanBP2, thereby inhibiting NR5A2 SUMOylation, ubiquitination, and subsequent degradation. Furthermore, the clinical data of HCC patients revealed two distinct HCC subtypes: high and low gp96

expression, which is positively correlated with serum AFP levels. Considering that AFP is the most widely used biomarker in HCC diagnosis and prognosis, our data provide new insights into the regulatory network of AFP expression and might help in designing more precise monitoring approaches for HCC diagnosis and progression.

## Materials and methods

### Animal studies

Liver-specific gp96KO mice were presented by Professor Zihai Li and generated by crossing Albumin-Cre mice with Hsp90b1flox/flox mice to obtain Albumin-Cre Hsp90b1flox/flox mice(Rachidi et al., 2015). Genotyping was done by PCR analysis of genomic DNA obtained from the tail, and the primer sequences used were 5'-TGCCAGAGACTACAATTCCCAGCA-3',5'-AAACACGAACTCACCAATCGT GCC-3' (Hsp90b1flox/flox mice), 5'-TGG CAA ACA TAC GCA AGG G-3', and 5'-CGG CAA ACG GAC AGA AGC A-3' (Albumin-Cre mice). Fifteen days after birth, gp96 KO and heterozygous (Het) mice were intraperitoneally injected with diethyl-nitrosamine (DEN) at a dose of 25 mg/kg. Mice were then sacrificed eight months after injection, and livers were excised. Externally visible tumors (≥ 1 mm) in the liver were counted and the liver tissues were stored at-80 °C. All animals received human care, and the mice study was in strict accordance with the "Institute of Microbiology, Chinese Academy of Sciences of Research Ethics Committee". The mice study protocol was approved by the Research Ethics Committee (permit number PZIMCAS2011001).

### Molecular modeling docking

The crystal structures of NR5A2 LBD (ligand-binding domain) from the docking model of NR5A2 DBD (DNA binding domain)-LBD, were obtained from PDB-Dev (PDBDEV_00000035)(Seacrist et al., 2020). The crystal structure of full-length gp96 (PDB code 5ULS, residues 48-754) contained three major domains: the N-terminal,

middle, and C-terminal domains(Huck et al., 2017). The crystal structure of the SUMO-RanGAP1-Ubc9-Nup358 complex has been reported previously (PDB code 1Z5S) containing RanBP2 residues 2631-2711(Reverter and Lima, 2005; Gareau et al., 2012). The gp96-NR5A2 and NR5A2-RanBP2 protein-protein docking models were created with ZDOCK Server (version 3.0.2) protein-protein docking; each with a centroid phase with rigid-body docking and an all-atom phase(Pierce et al., 2011). PyMoL was used for further visualization and figure preparation.

**Patient sample and specimens**

Paraffin-embedded hepatic tumor sections of 63 HCC patients were obtained from Department of Pathology and Hepatology, the fifth Medical Centre, Chinese PLA General Hospital, between January 2019 and August 2020. The studied clinical characteristics of the subjects are listed in Table 1. The serological AFP level included in this analysis was obtained from the preoperative measurement before and closest to the date of resection. The endogenous gp96 staining was categorized as low (score 1+), medium (score 2+), and high (score 3+) expression based on the staining intensity and immune reactive cell percentage according to a widely used scoring method (slightly modified)(Hicks and Tubbs, 2005). The intracellular g96 scoring is described as follows: score (+), slight and incomplete cell staining of hepatoma cells; Score (2+), medium cytoplasm staining in at least 50% of hepatocyte cells; Score (3+), high cytoplasm staining in at least 85% of hepatocyte cells. The assessments were blindly scored by two independent observers.

**Statistical analysis**

All data were analyzed using SPSS software (SPSS Science, Chicago, IL) and R software (version4.1.2; http://Rproject.org). Results are reported as the means ± standard deviations. Differences between mean values were analyzed using the Student's t-test. *P*-values < 0.05 were considered statistical significant.

## List of abbreviations

HCC, hepatocellular carcinoma; AFP, Alpha-fetoprotein; NR5A2, Nuclear receptor subfamily 5 group A member 2; DEN, diethyl-nitrosamine; TOP2A, DNA topoisomerase 2-alpha; HDAC4, Histone deacetylase 4; SIM, SUMO-interactive motif; DBD, DNA binding domain; LBD, ligand-binding domain; HNF-1, Hepatocyte Nuclear Factor-1; RXR, Retinoid x receptor; C/EBP, CAAT/enhancer binding protein; Nkx2.8, Homeobox protein NK-2; Zhx2, Zinc-fingers and homeoboxes 2; Zbtb20, Zinc finger and BTB domain containing 20.

**Acknowledgments**

The authors thank Donghong Wang, Xiuge Hou, Zihao Wang, Han Zhang, Yang Li, Xiaolan Zhang, Tong Zhao, Fang Cheng, Shuman Xie from Institute of Microbiology, Chinese Academy of Sciences for technical help and advices.

**Funding**

This work is supported by the funding from: a grant from the Strategic Priority Research Program of the Chinese Academy of Sciences (XDB29040000), the Industrial innovation team grant from Foshan Industrial Technology Research Institute, Chinese Academy of Sciences, the National Natural Science Foundation of China (32070163,81871297,81903142), the China ATOMIC energy authority, Foshan High-level Hospital construction DengFeng plan and Guangdong Province biomedical

innovation platform construction project tumor immunobiotherapy.

**Consent for publication**

Consent to publish has been obtained from all authors.

**Availability of data and materials**

The datasets used and analyzed during the current study are available from the corresponding authors on reasonable request.

**Competing interests**

The authors declare that there are no conflicts of interest.

**Authors' contributions**

S.M, L.Q, and C.L. concepted and designed the study. L.Q, and Z.L performed the experiments. L.Q, and Z.L collected data and samples. L.Q, S.M and C.L. made the statistical analysis and wrote the manuscript. C.L. and S.M supervised this work. All authors read and approved the final manuscript.

## References


Ansa-Addo, E.A., Thaxton, J., Hong, F., et al. (2016). Clients and Oncogenic Roles of Molecular Chaperone gp96/grp94. Curr Top Med Chem *16*, 2765-2778.

Bernier, D., Thomassin, H., Allard, D., et al. (1993). Functional analysis of developmentally regulated chromatin-hypersensitive domains carrying the alpha 1-fetoprotein gene promoter and the albumin/alpha 1-fetoprotein intergenic enhancer. Mol Cell Biol *13*, 1619-1633.

Berry, K., and Ioannou, G.N. (2013). Serum alpha-fetoprotein level independently predicts posttransplant survival in patients with hepatocellular carcinoma. Liver Transpl *19*, 634-645.

Blondel-Tepaz, E., Leverve, M., Sokrat, B., et al. (2021). The RanBP2/RanGAP1-SUMO complex gates β-arrestin2 nuclear entry to regulate the Mdm2-p53 signaling axis. Oncogene *40*, 2243-2257.

Chen, W., Peng, J., Ye, J., et al. (2020). Aberrant AFP expression characterizes a subset of hepatocellular carcinoma with distinct gene expression patterns and inferior prognosis. J Cancer *11*, 403-413.

Chen, W.T., Tseng, C.C., Pfaffenbach, K., et al. (2014). Liver-specific knockout of GRP94 in mice disrupts cell adhesion, activates liver progenitor cells, and accelerates liver tumorigenesis. Hepatology *59*, 947-957.

Cho, Y.B., Kim, J.W., Heo, K., et al. (2022). An internalizing antibody targeting of cell surface GRP94 effectively suppresses tumor angiogenesis of colorectal cancer. Biomed Pharmacother *150*, 113051.

Dawlaty, M.M., Malureanu, L., Jeganathan, K.B., et al. (2008). Resolution of sister centromeres requires RanBP2-mediated SUMOylation of topoisomerase IIalpha. Cell *133*, 103-115.

Delphin, C., Guan, T., Melchior, F., et al. (1997). RanGTP targets p97 to RanBP2, a filamentous protein localized at the cytoplasmic periphery of the nuclear pore complex. Mol Biol Cell *8*, 2379-2390.

Deutsch, H.F. (1991). Chemistry and biology of alpha-fetoprotein. Adv Cancer Res *56*, 253-312.

Duan, X., Iwanowycz, S., Ngoi, S., et al. (2021). Molecular Chaperone GRP94/GP96 in Cancers: Oncogenesis and Therapeutic Target. Front Oncol *11*, 629846.

Fan, H., Yan, X., Zhang, Y., et al. (2013). Increased expression of Gp96 by HBx-induced NF-κB activation feedback enhances hepatitis B virus production. PLoS One *8*, e65588.

Fan, Q., Mao, H., Wu, C., et al. (2014). ATF4 (activating transcription factor 4) from grass carp (Ctenopharyngodon idella) modulates the transcription initiation of GRP78 and GRP94 in CIK cells. Fish Shellfish Immunol *38*, 140-148.

Fayard, E., Auwerx, J., and Schoonjans, K. (2004). LRH-1: an orphan nuclear receptor involved in development, metabolism and steroidogenesis. Trends Cell Biol *14*, 250-260.

Galle, P.R., Foerster, F., Kudo, M., et al. (2019). Biology and significance of alpha-fetoprotein in hepatocellular carcinoma. Liver Int *39*, 2214-2229.

Gao, R., Cai, C., Gan, J., et al. (2015). miR-1236 down-regulates alpha-fetoprotein, thus causing PTEN accumulation, which inhibits the PI3K/Akt pathway and malignant phenotype in hepatoma cells. Oncotarget *6*, 6014-6028.

Gareau, J.R., Reverter, D., and Lima, C.D. (2012). Determinants of small ubiquitin-like modifier 1 (SUMO1) protein specificity, E3 ligase, and SUMO-RanGAP1 binding activities of nucleoporin RanBP2. J Biol Chem *287*, 4740-4751.

Gurakar, A., Ma, M., Garonzik-Wang, J., et al. (2018). Clinicopathological Distinction of

Low-AFP-Secreting vs. High-AFP-Secreting Hepatocellular Carcinomas. Ann Hepatol *17*, 1052-1066.

Hicks, D.G., and Tubbs, R.R. (2005). Assessment of the HER2 status in breast cancer by fluorescence in situ hybridization: a technical review with interpretive guidelines. Hum Pathol *36*, 250-261.

Hong, F., Liu, B., Chiosis, G., et al. (2013). α7 helix region of αI domain is crucial for integrin binding to endoplasmic reticulum chaperone gp96: a potential therapeutic target for cancer metastasis. J Biol Chem *288*, 18243-18248.

Hoter, A., El-Sabban, M.E., and Naim, H.Y. (2018). The HSP90 Family: Structure, Regulation, Function, and Implications in Health and Disease. Int J Mol Sci *19*.

Hou, J., Deng, M., Li, X., et al. (2015a). Chaperone gp96 mediates ER-α36 cell membrane expression. Oncotarget *6*, 31857-31867.

Hou, J., Li, X., Li, C., et al. (2015b). Plasma membrane gp96 enhances invasion and metastatic potential of liver cancer via regulation of uPAR. Mol Oncol *9*, 1312-1323.

Huck, J.D., Que, N.L., Hong, F., et al. (2017). Structural and Functional Analysis of GRP94 in the Closed State Reveals an Essential Role for the Pre-N Domain and a Potential Client-Binding Site. Cell Rep *20*, 2800-2809.

Ji, F., Zhang, Y., Zhu, Z.B., et al. (2019). Low levels of glycoprotein 96 indicate a worse prognosis in early-stage hepatocellular carcinoma patients after hepatectomy. Hum Pathol *86*, 193-202.

Kajiyama, Y., Tian, J., and Locker, J. (2006). Characterization of distant enhancers and promoters in the albumin-alpha-fetoprotein locus during active and silenced expression. J Biol Chem *281*, 30122-30131.

Kim, J.W., Cho, Y.B., and Lee, S. (2021). Cell Surface GRP94 as a Novel Emerging Therapeutic Target for Monoclonal Antibody Cancer Therapy. Cells *10*.

Kirsh, O., Seeler, J.S., Pichler, A., et al. (2002). The SUMO E3 ligase RanBP2 promotes modification of the HDAC4 deacetylase. Embo j *21*, 2682-2691.

Kojima, K., Takata, A., Vadnais, C., et al. (2011). MicroRNA122 is a key regulator of α-fetoprotein expression and influences the aggressiveness of hepatocellular carcinoma. Nat Commun *2*, 338.

Koo, B.H., and Apte, S.S. (2010). Cell-surface processing of the metalloprotease pro-ADAMTS9 is influenced by the chaperone GRP94/gp96. J Biol Chem *285*, 197-205.

Lee, J., Yang, D.J., Lee, S., et al. (2016). Nutritional conditions regulate transcriptional activity of SF-1 by controlling sumoylation and ubiquitination. Sci Rep *6*, 19143.

Li, X., Sun, L., Hou, J., et al. (2015). Cell membrane gp96 facilitates HER2 dimerization and serves as a novel target in breast cancer. Int J Cancer *137*, 512-524.

Liu, B., Yang, Y., Qiu, Z., et al. (2010). Folding of Toll-like receptors by the HSP90 paralogue gp96 requires a substrate-specific cochaperone. Nat Commun *1*, 79.

Liu, W., Zeng, M., and Fu, N. (2021a). Functions of nuclear receptors SUMOylation. Clin Chim Acta *516*, 27-33.

Liu, X., Chen, X., Xiao, M., et al. (2021b). RANBP2 Activates O-GlcNAcylation through Inducing CEBPα-Dependent OGA Downregulation to Promote Hepatocellular Carcinoma Malignant Phenotypes. Cancers (Basel) *13*.

Liu, X., Liu, J., Xiao, W., et al. (2020). SIRT1 Regulates N(6) -Methyladenosine RNA Modification in Hepatocarcinogenesis by Inducing RANBP2-Dependent FTO SUMOylation. Hepatology *72*, 2029-2050.

Marzec, M., Eletto, D., and Argon, Y. (2012). GRP94: An HSP90-like protein specialized for protein folding and quality control in the endoplasmic reticulum. Biochim Biophys Acta *1823*, 774-787.

Marzec, M., Hawkes, C.P., Eletto, D., et al. (2016). A Human Variant of Glucose-Regulated Protein 94 That Inefficiently Supports IGF Production. Endocrinology *157*, 1914-1928.

Niu, M., Xu, J., Liu, Y., et al. (2021). FBXL2 counteracts Grp94 to destabilize EGFR and inhibit EGFR-driven NSCLC growth. Nat Commun *12*, 5919.

Peterson, M.L., Ma, C., and Spear, B.T. (2011). Zhx2 and Zbtb20: novel regulators of postnatal alpha-fetoprotein repression and their potential role in gene reactivation during liver cancer. Semin Cancer Biol *21*, 21-27.

Pichler, A., Gast, A., Seeler, J.S., et al. (2002). The nucleoporin RanBP2 has SUMO1 E3 ligase activity. Cell *108*, 109-120.

Pierce, B.G., Hourai, Y., and Weng, Z. (2011). Accelerating protein docking in ZDOCK using an advanced 3D convolution library. PLoS One *6*, e24657.

Piñero, F., Dirchwolf, M., and Pessôa, M.G. (2020). Biomarkers in Hepatocellular Carcinoma: Diagnosis, Prognosis and Treatment Response Assessment. Cells *9*.

Pugh, K.W., Alnaed, M., Brackett, C.M., et al. (2022). The biology and inhibition of glucose-regulated protein 94/gp96. Med Res Rev *42*, 2007-2024.

Rachidi, S., Sun, S., Wu, B.X., et al. (2015). Endoplasmic reticulum heat shock protein gp96 maintains liver homeostasis and promotes hepatocellular carcinogenesis. J Hepatol *62*, 879-888.

Reverter, D., and Lima, C.D. (2005). Insights into E3 ligase activity revealed by a SUMO-RanGAP1-Ubc9-Nup358 complex. Nature *435*, 687-692.

Rosonina, E., Akhter, A., Dou, Y., et al. (2017). Regulation of transcription factors by sumoylation. Transcription *8*, 220-231.

Sauzay, C., Petit, A., Bourgeois, A.M., et al. (2016). Alpha-foetoprotein (AFP): A multi-purpose marker in hepatocellular carcinoma. Clin Chim Acta *463*, 39-44.

Seacrist, C.D., Kuenze, G., Hoffmann, R.M., et al. (2020). Integrated Structural Modeling of Full-Length LRH-1 Reveals Inter-domain Interactions Contribute to Receptor Structure and Function. Structure *28*, 830-846.e839.

Shi, B., Lu, H., Zhang, L., et al. (2018). A homologue of Nr5a1 activates cyp19a1a transcription additively with Nr5a2 in ovarian follicular cells of the orange-spotted grouper. Mol Cell Endocrinol *460*, 85-93.

Sun, Y., Demagny, H., and Schoonjans, K. (2021). Emerging functions of the nuclear receptor LRH-1 in liver physiology and pathology. Biochim Biophys Acta Mol Basis Dis *1867*, 166145.

Trevisani, F., D'Intino, P.E., Morselli-Labate, A.M., et al. (2001). Serum alpha-fetoprotein for diagnosis of hepatocellular carcinoma in patients with chronic liver disease: influence of HBsAg and anti-HCV status. J Hepatol *34*, 570-575.

Werner, A., Flotho, A., and Melchior, F. (2012). The RanBP2/RanGAP1*SUMO1/Ubc9 complex is a multisubunit SUMO E3 ligase. Mol Cell *46*, 287-298.

Wu, B., Chu, X., Feng, C., et al. (2015). Heat shock protein gp96 decreases p53 stability by regulating Mdm2 E3 ligase activity in liver cancer. Cancer Lett *359*, 325-334.

Wu, B.X., Hong, F., Zhang, Y., et al. (2016). GRP94/gp96 in Cancer: Biology, Structure, Immunology, and Drug Development. Adv Cancer Res *129*, 165-190.

Xie, Z., Zhang, H., Tsai, W., et al. (2008). Zinc finger protein ZBTB20 is a key repressor of

alpha-fetoprotein gene transcription in liver. Proc Natl Acad Sci U S A *105*, 10859-10864.

Xue, J., Cao, Z., Cheng, Y., et al. (2020). Acetylation of alpha-fetoprotein promotes hepatocellular carcinoma progression. Cancer Lett *471*, 12-26.

Zheng, Y., Zhu, M., and Li, M. (2020). Effects of alpha-fetoprotein on the occurrence and progression of hepatocellular carcinoma. J Cancer Res Clin Oncol *146*, 2439-2446.

**Table 1**

**The associated of gp96 protein level with Serum AFP levels in patients with primary HCC**

| characteristic | Gp96 expression | | *P* value |
|---|---|---|---|
| | Low(13/63) | High(50/63) | |
| Age(years) | | | 0.5018 |
| <50 | 6 | 18 | |
| >=50 | 7 | 32 | |
| | | | |
| Gender | | | 0.2699 |
| male | 12 | 38 | |
| Female | 1 | 12 | |
| | | | |
| Tumor size | | | 0.5078 |
| <3cm | 5 | 14 | |
| >=3cm | 8 | 36 | |
| | | | |
| Tumor number | | | 0.739 |
| =1 | 8 | 35 | |
| >1 | 5 | 15 | |

| | | | |
|---|---|---|---|
| | | | |
| HBsAg | | | 0.1893 |
| Positive | 6 | 33 | |
| Negative | 7 | 17 | |
| | | | |
| | | | |
| HBcAg | | | 0.8006 |
| Positive | 1 | 5 | |
| Negative | 12 | 45 | |
| | | | |
| T stage | | | 0.2063 |
| I-II | 1 | 0 | |
| III-IV | 12 | 50 | |
| | | | |
| Differentiation grade | | | 0.631 |
| Well differentiated | 0 | 3 | |
| Moderatedly differentiated | 12 | 42 | |
| Poorly differentiated | 1 | 5 | |
| | | | |
| Extrahepatic spread | | | NA |
| Yes | 0 | 0 | |
| No | 13 | 50 | |

| | | | |
|---|---|---|---|
| Recurrence | | | NA |
| positive | 0 | 0 | |
| negative | 13 | 50 | |

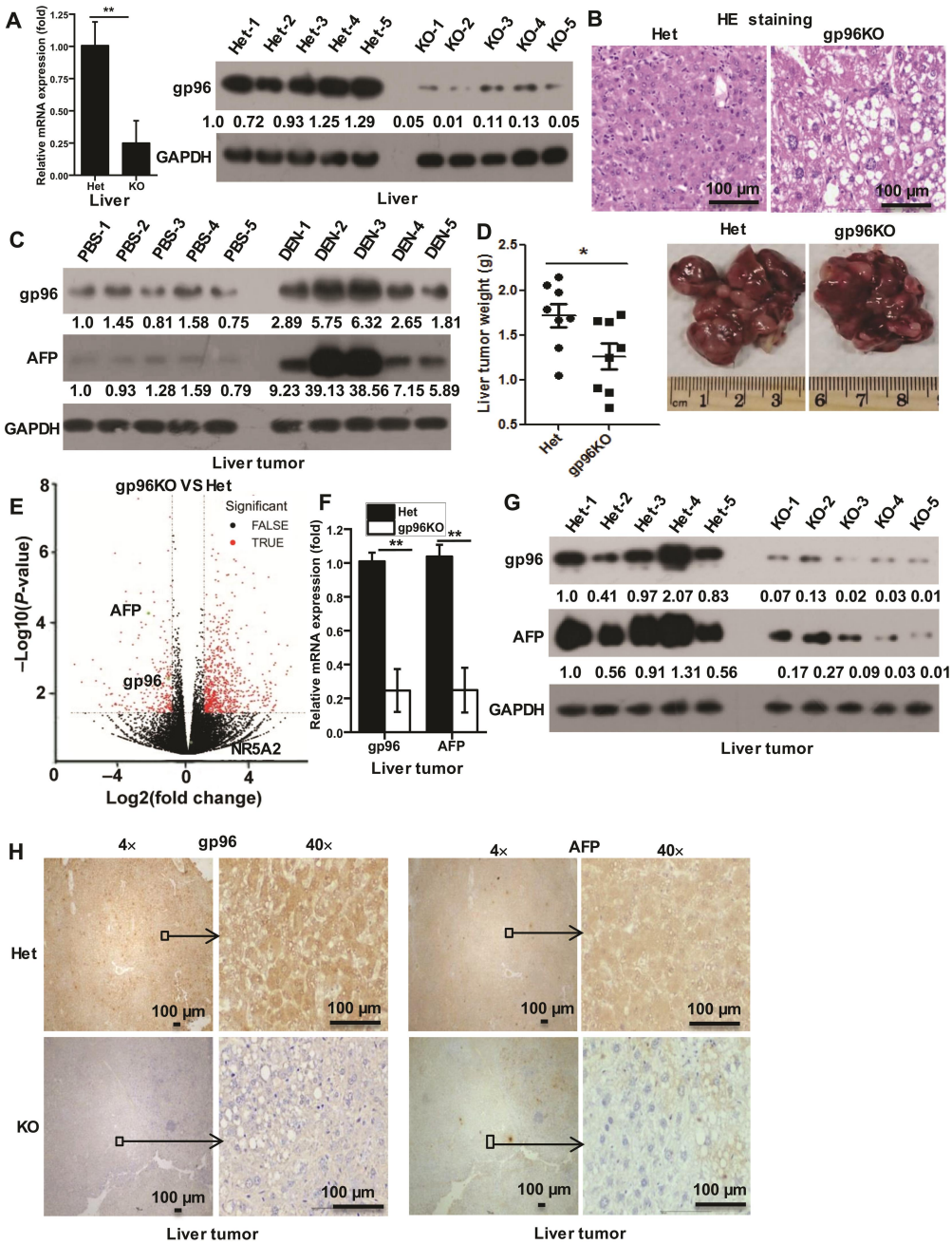


**Figure 1**

**Figure 1 AFP expression analysis in the liver tumor of hepatic gp96KO mice.** (A) Representative section photographs, Real-time PCR, and Western blot analysis of mRNA and protein levels gp96 and AFP in the normal liver of Het and gp96KO mice (n = 5/group). (B) Representative photographs and HE-staining of liver tumors in

DEN-treated Het and gp96KO mice. (C) Western blot analysis of gp96 and AFP in tumor and normal liver tissues of DEN-treated Het and PBS-treated mice, respectively. (D) Mass of Het and KO mice livers after eight months of DEN treatment. (E) Microarray volcano map of differently expressed genes in hepatic tumors of gp96KO and Het mice (control) treated with DEN. (Fand G) Real-time PCR (F) and Western blot (G) analysis of gp96 and AFP mRNA and protein levels in the liver tumors of Het and gp96KO mice (n = 5/group). (H) IHC analysis of gp96 (left panel) and AFP (right panel) expression in paraffin tumor tissue sections of Het and gp96KO mice. $^{**}P < 0.01$, compared with the control group.

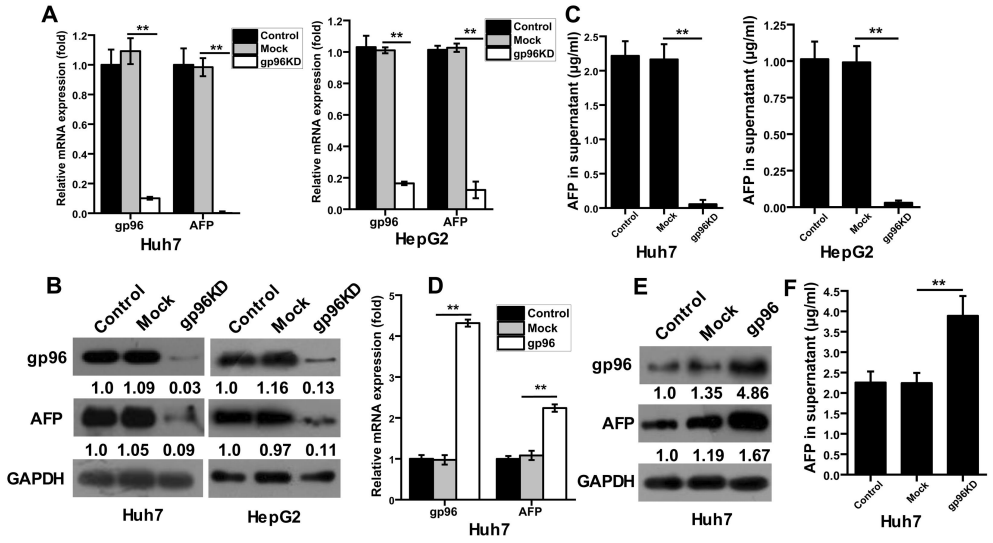


**Figure 2**

**Figure 2 Effect of gp96 knockdown or overexpression on AFP levels in hepatoma cell lines.** (A-C) Huh7 and HepG2 cells were stably transfected with gp96 shRNA (gp96KD) or luciferase shRNA (Luci) as mock, or untransfected as control. Cellular AFP levels were detected by Real-time PCR (A) and Western blotting (B). AFP levels in cell supernatant were analyzed by ELISA(C). (D-F) Huh7 cells were stably transfected with gp96 vector or empty vector as mock. Cellar mRNA and protein levels of AFP were determined by Real-time PCR (D) and Western blotting (E), and AFP levels in cell supernatant were measured by ELISA (F). Data are presented as the means ±SD from three independent experiments. $^{**}P < 0.01$ compared to the mock.

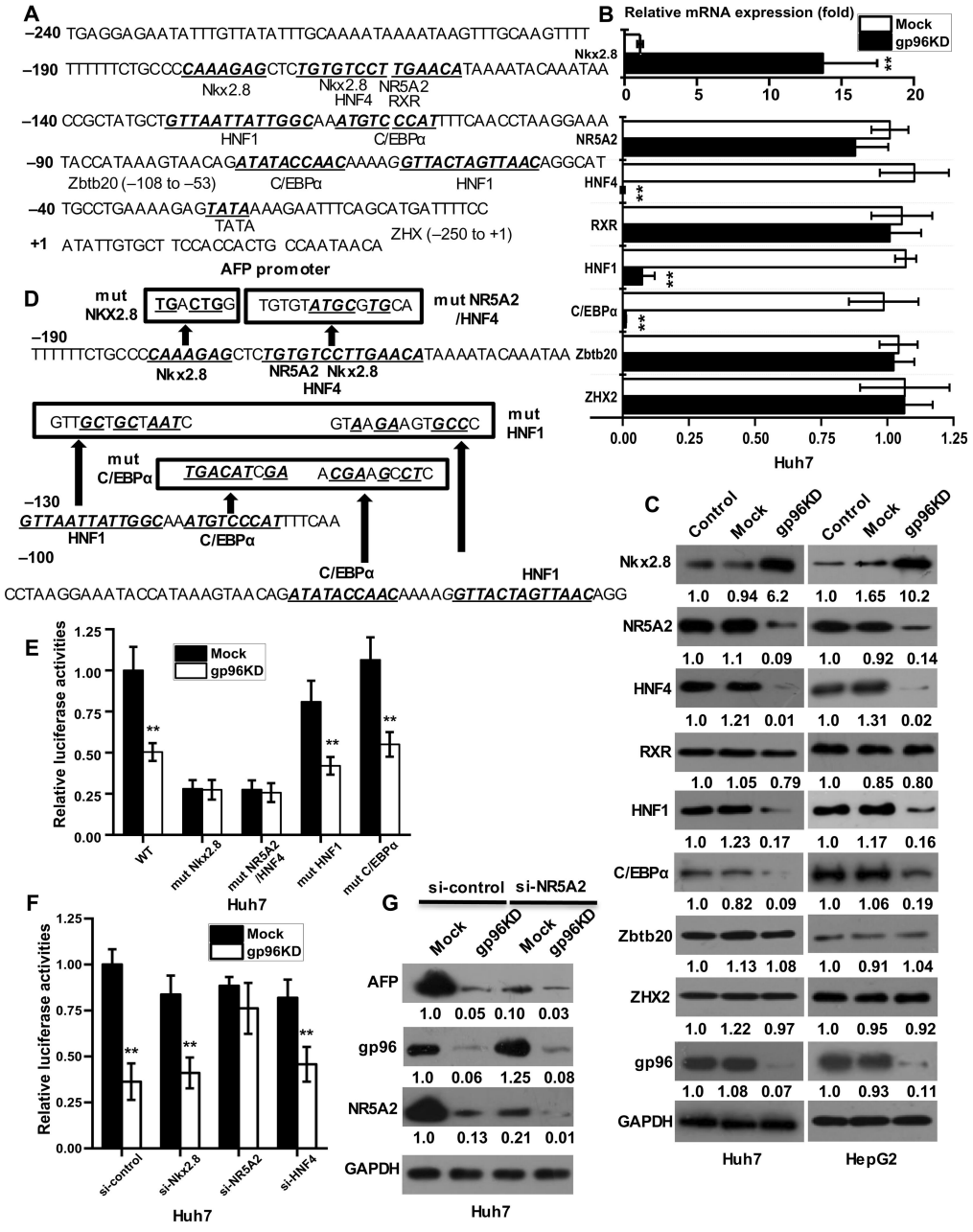


**Figure 3**

**Figure 3 Identification of NR5A2 as a key transcription factor in gp96-induced AFP expression.** (A) The putative binding sites in the AFP promoter for its transcription factors were defined using italics, bold letters, and underlining. (B andC) Levels of AFP transcription factors were assessed by Real-time PCR (B) and Western

blotting (C) in Huh7 and HepG2 cells, similar to Figure (2A-2C). (D)The mutant binding sequences of AFP transcription factors in its promoter were shown in italics and bold letters in boxes. (E) Huh7-gp96KD or and Huh7-Luci (mock) cells were co-transfected with an empty pGL3-Basic construct (control), the pGL3-Basic construct containing wild-type AFP promoter (-240/+29) (pAFP-Luci, WT), or pAFP-Luci with mutant AFP promoter within the binding sites of Nkx2.8, NR5A2/HNF4, HNF1 or C/EBPα, and pRL-TK. AFP promoter and Renilla luciferase activities were measured at 48 h after transfection. The luciferase activity of Huh7-Luci cells transfected with WT pAFP-Luci was set as 1.0. (F) Huh7-gp96KD (Huh7-Luci as mock) cells were co-transfected with the siRNA of control (si-control ) or Nkx2.8 (si-Nkx2.8) or NR5A2 (si-NR5A2) or HNF4 (si-HNF4), pAFP-Luci, and pRL-TK. AFP promoter and Renilla luciferase activities were examined at 48 h after transfection. The luciferase activity of Huh7-Luci cells transfected with control siRNA (si-control) was set as 1.0. Huh7-gp96KD and Huh7-Luci (mock) cells were co-transfected with the siRNA of NR5A2 (si-NR5A2) or control (si-control) as mock. Cellular AFP levels were detected by Western blotting (G). Data are presented as the means ±SD from three independent experiments. $*P < 0.05$ and $**P < 0.01$ compared to the mock.

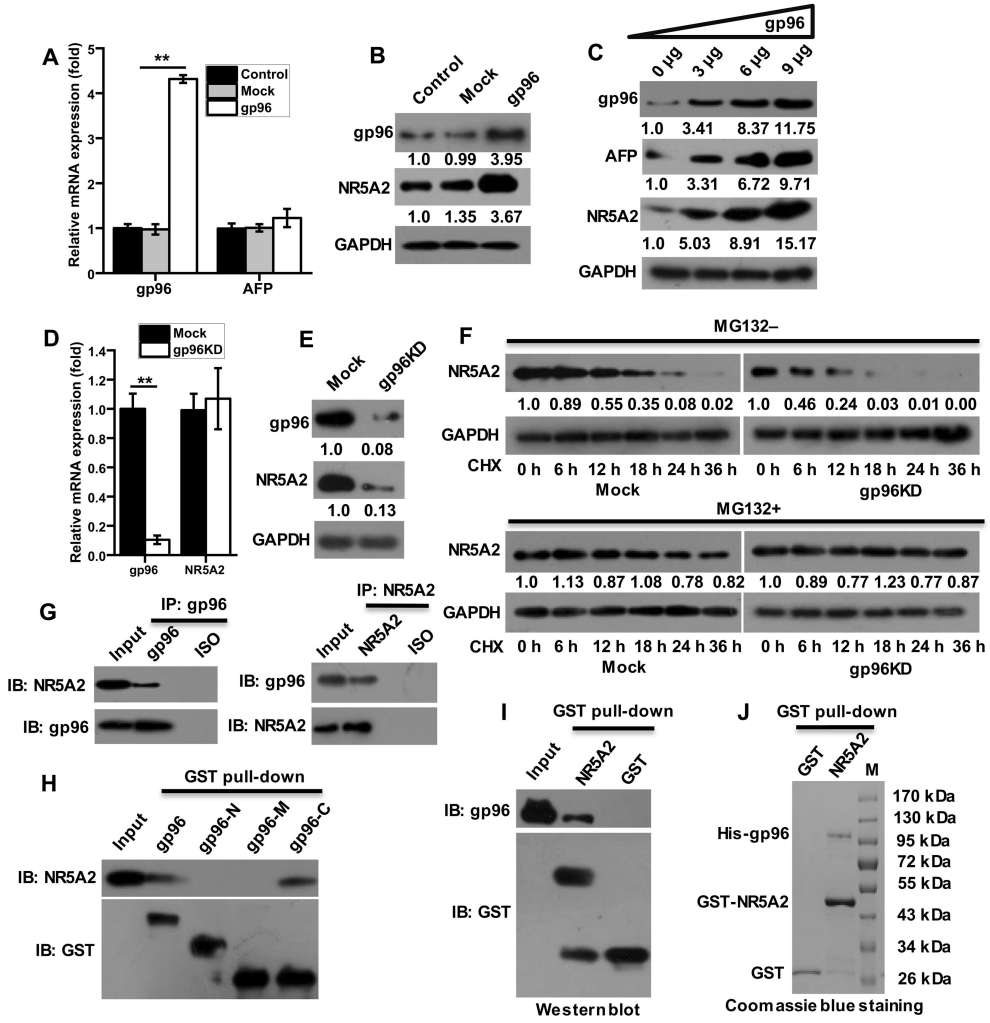


**Figure 4**

**Figure 4 Effect of cellular gp96 on NR5A2 protein stability and their interaction.** (A,B,D,E) NR5A2 mRNA and protein levels were measured by Real-time PCR (A and D) and Western blotting (B and E) in Huh7 cells stably transfected with gp96 expression vector (Huh7-gp96) or empty vector as mock or un-transfected as control (A andB), or in Huh7-gp96KD or Huh7-luci as mock. (C) Huh7 cells were transfected with increasing amounts (0, 3, 6, 9 μg) of pcDNA3.1-gp96. At 48 h post-transfection, AFP and NR5A2 levels were determined by western blot. (F) Huh7-gp96KD or Huh7-Luci mock cells were treated with 50 μM CHX alone for the indicated times or together with 20 μM MG132. NR5A2 protein levels were analyzed by Western

blotting. (G) The co-IP assay was performed with anti-gp96 or anti-NR5A2 monoclonal antibody, in Huh7 cells, and IgG as isotype (ISO) control. The immunoprecipitates were immunoblotted with specific antibodies. (H) Huh7 cell lysates were incubated with equal amounts of GST-gp96 (aa22-803), its gp96-N (aa22-376), gp96-M (aa337-594), or gp96-C(aa561-803) terminal fragment for 3 h followed by incubation with GST beads overnight at 4 °C. The pull-down materials were immunoblotted for NR5A2. (I) GST-gp96 or GST-C terminal protein was incubated recombinant NR5A2 (aa 299-536), and the GST pull-down materials were subjected to SDS-PAGE analysis. (J)GST-NR5A2 (aa 299-536) and GST protein was incubated recombinant His-gp96, and GST pull-down materials were subjected to Coomassie blue analysis. Data are presented as the means ±SD from three independent experiments. $^{**}P < 0.01$ compared to the mock.

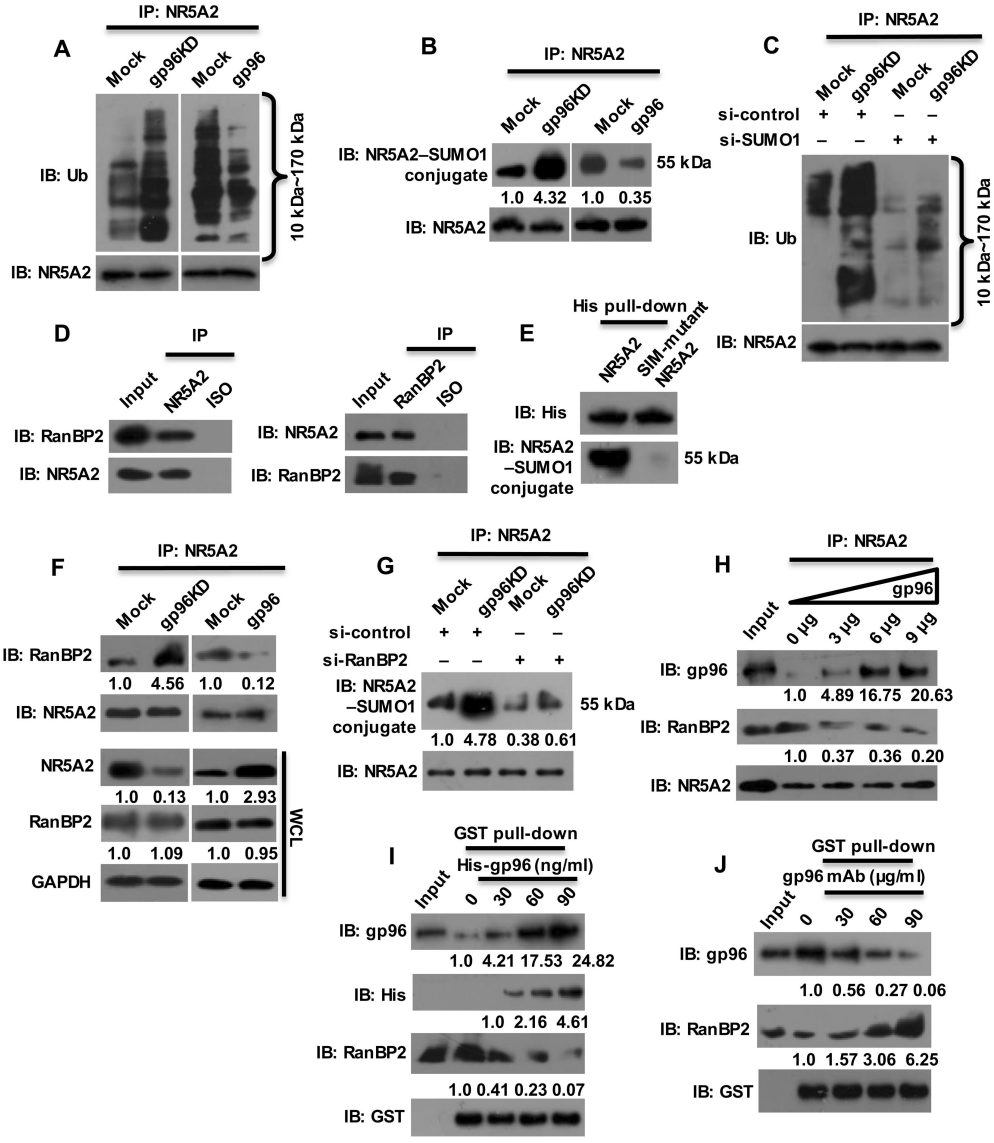


**Figure 5**

**Figure 5 Regulation of RanBP2-mediated NR5A2 SUMOylation and subsequent ubiquitination by gp96.** (A and B) Huh7-gp96KD, Huh7-gp96, or mock cells were exposed to 20 μM MG132 or 20 μM NEM for 6 h before lysis. NR5A2 protein was immunoprecipitated and subjected to immunoblot with an antibody specific to ubiquitin (A) or SUMO1 (B). (C) Huh7-gp96KD and mock cells were transfected with SUMO1 siRNA (si-SUMO1) or control siRNA (si-control). At 48 h after

transfection, cells were lysed and ubiquitination of NR5A2 was analyzed. (D) Co-IP experiments were performed with anti-NR5A2 (left) or anti-RanBP2 (right) antibody and IgG as the isotype (ISO) control. The immunoprecipitates were immunoblotted with specific antibodies. (E) Huh7 cells were transfected with pcDNA3.1-his-WT NR5A2 or pcDNA3.1-his-SIM mutant NR5A2. At 48 h post-transfection, cell lysates were incubated with Ni-NTA Sepharose beads for 2~3 h followed by detection of His-tag and SUMO1 by western blotting. (F) NR5A2 was immunoprecipitated with NR5A2 antibody from lysates of Huh7-gp96KD or Huh7-gp96 cells, respectively. RanBP2 in the immunoprecipitates was assessed by Western blotting. Whole-cell lysates (WCL) were also blotted for respective proteins. (G) Huh7-gp96KD cells were transfected with RanBP2 siRNA (si-RanBP2) or control siRNA (si-control). At 48 h after transfection, NR5A2 was immunoprecipitated from cell lysates followed by SUMO1 detection by Western blotting. (H) Huh7 cells were transfected with increasing amounts (0, 3, 6, 9 μg) of pcDNA3.1-gp96. At 48 h post-transfection, NR5A2 was immunoprecipitated with NR5A2 antibody, followed by the Western blotting analysis of RanBP2 in the complexes. (I and J) Cell lysates of Huh7 were treated with the indicated amounts of his-gp96 (I) or gp96 antibody (J), and an equal amount of GST-NR5A2 was added for 3 h, followed by incubation with GST beads overnight. The pull-down materials were immunoblotted for gp96, His, RanBP2, or GST. All experiments were performed at least twice with similar results.

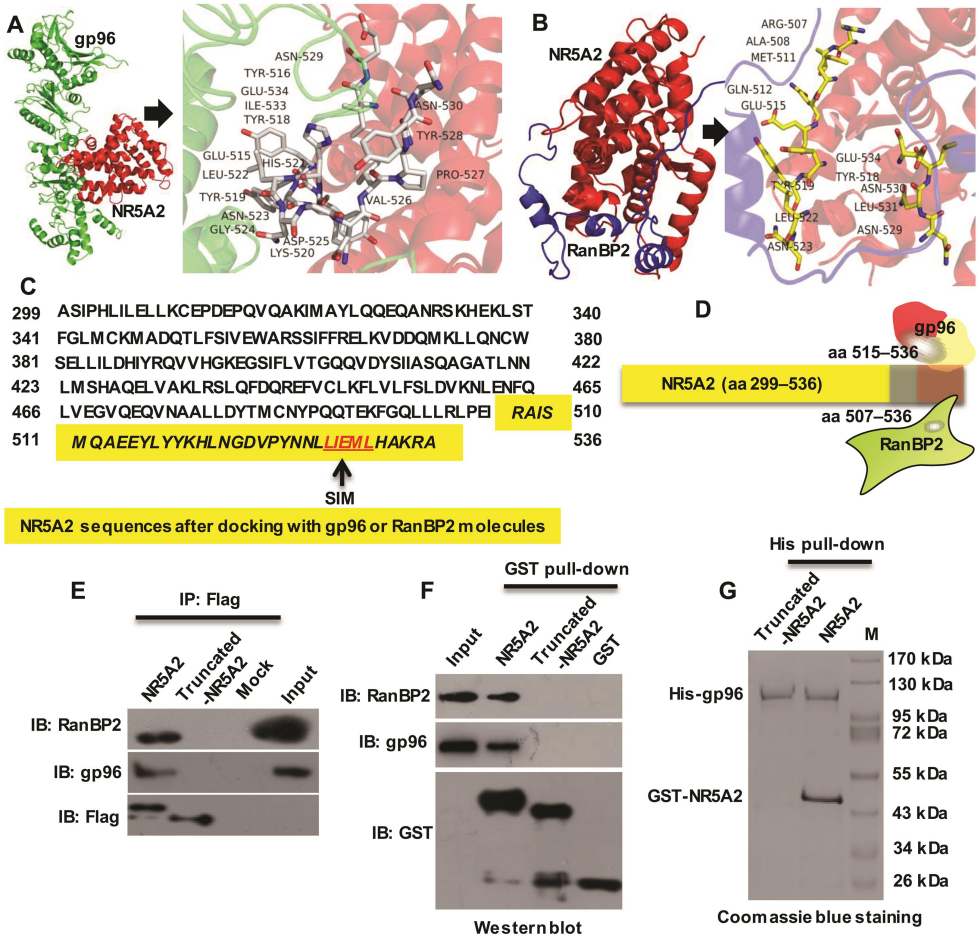


**Figure 6**

**Figure 6 Analysis of the binding sites of gp96 and RanBP2 in NR5A2.** (Aand B) Cartoon representation of gp96 (A) or RanBP2 (B) docking model with NR5A2. Gp96, RanBP2, and NR5A2 residues are colored in green, blue, and red, respectively. The interaction amino acids between gp96 or RanBP2 and NR5A2 were shown as white or yellow sticks, and non-carbon atoms are colored according to their chemical identity (C, white or yellow; O, red; N, blue; H, wheat). (C) The amino acid sequence of NR5A2 (aa 299-536). The putative binding sites in the NR5A2 LBDregions for gp96 or RanBP2 were underlined in italics and bold letters. (D) The cartoon figure showing interaction regions in the NR5A2 LBDwith gp96 and RanBP2. (E) Huh7

cells were transfected with pcDNA3.1-Flag-NR5A2 (aa 299-536), pcDNA3.1-Flag-NR5A2 (aa 299-506), or empty vector as mock. At 48 h post-transfection, cell lysates were immunoprecipitated with Flag antibody followed by immunoblotting of RanBP2, gp96, and Flag. (F) *In vitro,* GST-pull down assay was performed with GST-NR5A2 (aa 299-536) or truncated GST-NR5A2 (aa 299-506) and Huh7 cell lysates, followed by immunoblotting of RanBP2, gp96, and GST. (G) Equal amounts of GST-NR5A2 (aa 299-536) or truncated GST-NR5A2 (aa 299-506) were incubated with His-gp96 and incubation with Ni-NTA Sepharose beads for 2 hours. His pull-down was assayed by Coomassie blue staining after resolution by 10% SDS–PAGE. All experiments were performed at least three times with similar results.

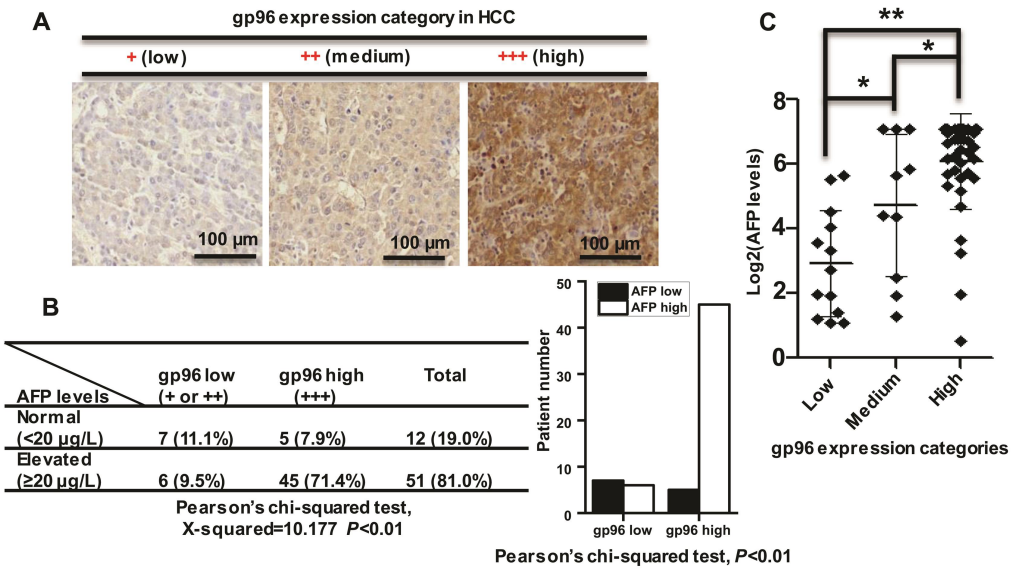


Figure 7

**Figure 7 Correlation of gp96 expression in tumors and serum AFP levels in HCC patients.** (A) IHC analysis of gp96 expression in primary HCC tissue. Representative images indicating immunostaining intensities of 1+, 2+, and 3+ are shown. (B) The correlation between gp96 expression and AFP levels in the serum of HCC patients was analyzed by Pearson's chi-squared test. Distribution of serum AFP levels in tumors with low, medium, and high gp96 expression. (C) Correlation between gp96 expression categories and higher serum AFP levels in the serum of HCC patients.

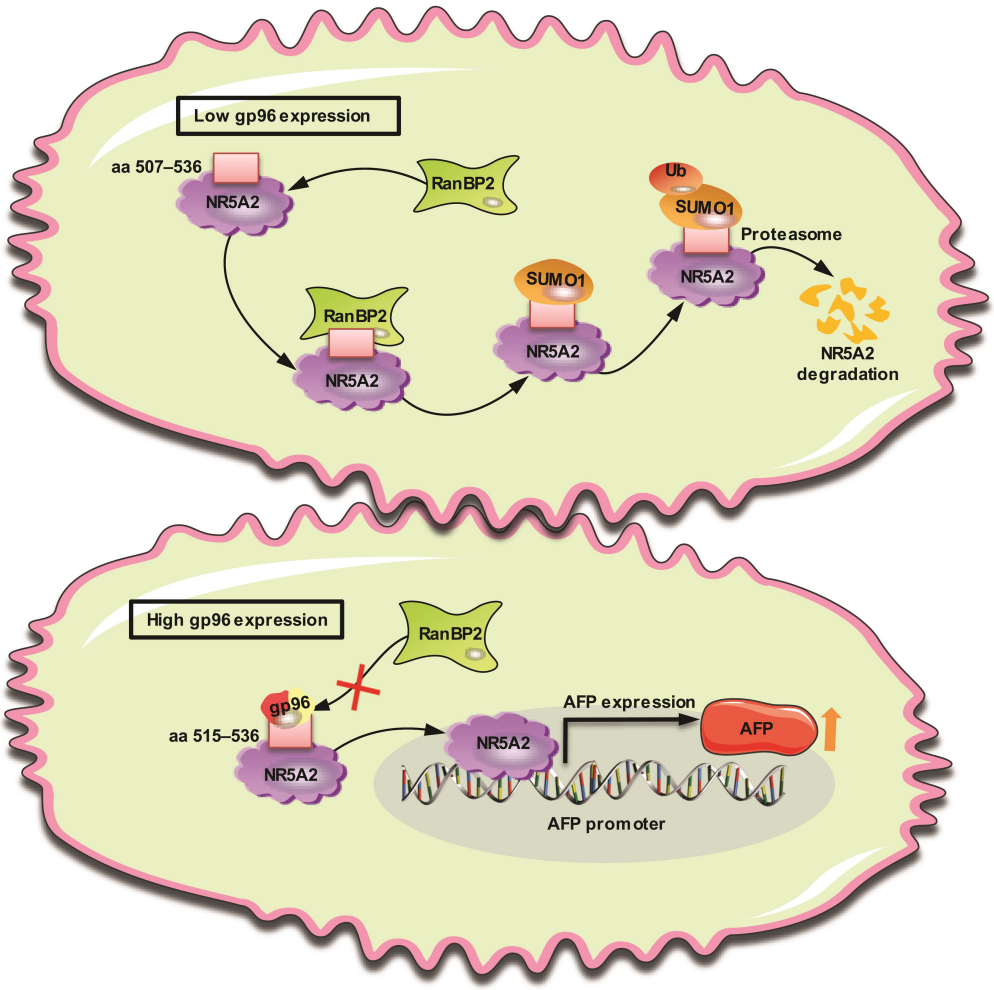


**Figure 8**

**Figure 8 Schematic figure of gp96 promoting AFP expression in HCC.** SUMOylation of NR5A2 by RanBP2 leads to its subsequent ubiquitination and proteasomal degradation. Cellular gp96, under its elevated expression in HCC, binds to NR5A2 at the site spanning from aa 507 to 536 which overlaps with the RanBP2 interaction site. The binding of gp96 sterically hinders the interaction of RanBP2 and NR5A2, thereby protecting NR5A2 from SUMOylation and degradation. Upregulated NR5A2 binds to the AFP promoter and enhances its expression.